CERN/MPS-MU/SD 70- 3
YB/ld - 18. 8.1970

SURFACE RESISTANCE MEASUREMENTS IN TE_{011} MODE CAVITIES OF SUPERCONDUCTING INDIUM, LEAD AND AN INDIUM-LEAD ALLOY AT LOW AND HIGH RF MAGNETIC FIELDS

(Paper to be submitted to Physica)

Y. Bruynseraede*, D. Gorle**, D. Leroy, P. Morignot***

*) CERN Research Associate, on leave of absence from Instituut voor Lage Temperaturen en Technische Fysica, Universiteit Leuven, 3030 Heverlee, Belgium;

**) Present address : Centre de Recherche Routier
1960 Sterrebeek, Belgium;

***) Present address : La Radiotechnique, 14 Caen, France.

PS/276

SUMMARY

The superconducting surface resistance of Pb, In and $In_{.92}Pb_{.08}$ was measured between 1.5 K and 4.2 K at low and high power levels in TE_{011} mode cavities resonating at 2.85 GHz. A residual surface resistance of 9.4×10^{-8} ohms was achieved in the lead-plated cavity corresponding to a Q of 8.3×10^{9}. It is shown that the microscopic theoretical expression for the superconducting surface resistance adequately describes the experimental results for Pb and In , both type-I superconductors, and for $In_{.92}Pb_{.08}$, a type-II superconductor. In lead and indium-plated cavities, and if heating effects are taken into account, the unloaded Q was observed to be essentially a constant up to the RF critical magnetic field B_c^{RF}, where it abruptly decreased by a factor of 100 or more. This transition is characterized by breakdown oscillation phenomena. An B_c^{RF} as large as 225 G for In and 750 G for Pb was observed.

Measurements as a function of temperature indicated that the RF critical magnetic field of In and Pb is in agreement with the DC critical magnetic field.

The largest measured B_c^{RF} ($\simeq$ 90 G) on the In-alloy disc is a factor 3 smaller than the lower DC critical magnetic field, $B_{c1}(1.5\ K) \simeq 270$ G .

TABLE OF CONTENTS

1. INTRODUCTION

It was experimentally shown that the microwave surface resistance at low power of Sn and Pb[1] - type-I superconductors - and of Nb[2] - type II superconductor - is adequately described by the microscopic theory[3]. For Sn, high power measurements indicated that the RF critical magnetic field is consistent with the DC critical magnetic field[1].

In the present work, measurements of the surface resistance at low and high power were carried out at 2.85 GHz on superconducting In and Pb layers and a massive $In_{.92}Pb_{.08}$-alloy disc. The experimental data are in agreement with the superconducting surface resistance calculated from the microscopic theory including the effects of a finite electron mean free path[1-4]. Measurements on In and Pb layers at high power levels, as a function of temperature, confirmed the results reported by Turneaure[1] for Sn : the RF critical magnetic field for these metals is equal to the thermodynamic critical field.

One of the principal goals of this work was however to compare the behaviour at high field levels of a type-I superconductor (In and Pb) and a type-II superconductor ($In_{.92}Pb_{.08}$-alloy). Due to heating effects it was not yet possible to obtain very high RF field values on the indium-alloy surface.

The first part of this report gives a description of the measuring and cavity preparation techniques. A comparison between the experimental data and the theoretical predictions is given in the second part. High power level measurements are discussed in the last section of this paper.

2. GENERAL EXPERIMENTAL TECHNIQUES

2.1. CAVITY PREPARATION

The surface resistance measurements were carried out on cylindrical test cavities resonating at 2.85 GHz in the TE_{011} mode (Fig. 1a). By choosing this mode, in which the current flow is circumferential[5], the problem of making good RF contacts between cylinder wall and end plates is minimized. Furthermore, this mode is suitable for analysing magnetic field phenomena since it has no electrical field on the surface which can produce electron field emission[6] or dielectric losses.

The cavity consists of three pieces : a cylinder and two end plates. At a fixed temperature, In and $In_{.92}Pb_{.08}$ have a higher superconducting surface resistance than Pb. Therefore, in order to reduce the dissipated power during the high field level measurements, one end plate and the cylinder wall are electroplated with lead, whereas the other end plate is covered with In or made of $In_{.92}Pb_{.08}$ (bottom plate in Fig. 1a).

The preparations of the indium and lead surfaces (electroplating) differed from the indium-lead alloy (machined from a single piece) and will be discussed separately.

2.1.1. Electroplated indium and lead surfaces

The three cavity pieces, made from HCOKOF-Copper (Outokumpu, Finland) are separately electroplated and subsequently assembled together with indium gaskets to be vacuum tight.

The preparation of the copper substrate as well as the lead plating technique has already been described in a previous report[7]. The plating solution and anode are respectively commercial grade lead fluoborate and purified lead (99.998 o/o).

The characteristics of the two indium electroplating solutions used in these studies are summarized in Table I.

TABLE 1

COMPOSITION	
Indium Fluoborate Bath*	Indium Sulfate Bath**
Indium Fluoborate ($In(BF_4)_3$) : 108 g/l Indium Metal Equivalent : 33 g/l Boric Acid (H_3BO_3) : 25 g/l Ammonium Fluoborate (NH_4BF_4) : 50 g/l	Indium Sulfate ($In_2(SO_4)_3$) : 90 g/l Indium Metal Equivalent: 20 g/l Sodium Sulfate (Na_2SO_4): 10 g/l

OPERATING CONDITIONS		
	Indium Fluoborate Bath	Indium Sulfate Bath
pH of the Bath	1.5 - 2.0	2.0 - 2.5
Bath temperature	~ 20 C	~ 20 C
Current density	0.5 - 2.5 A/dm^2	2 - 8 A/dm^2
Deposition time	~ 30 min.	~ 30 min.
Anode	In (99.99 o/o)	In (99.99 o/o)

* "Baker and Adamson", Trademark of the General Chemical Div. of Allied Chemical, N.Y., U.S.A.

** Supplied by Caplain, Paris, France

The impurity content of the bath was measured (spectro-photometer) for the ferromagnetic atoms iron and nickel. In general, the indium sulfate bath contained less than 0.01 o/o of these atoms, which is the detection sensitivity of the spectrometer.

The indium fluoborate solution however contained, probably by accident, approximately 10 mg/l Ni^{2+} and 0.5 mg/l Fe^{2+} atoms. Although no traces of nickel or iron were found in the electroplated indium layer, the superconducting properties of indium from the fluoborate bath are quite different from those observed for indium from the sulfate bath (see Sections 3 and 4).

After a layer of approximately 10 microns thick had been deposited, the cavity components are removed from the solution, rinsed and dried. Precautions are taken during these last two processes to avoid oxidization : rinsing in distilled water which is then expelled by an oxygen-free dry nitrogen gas jet and drying in vacuum. The cavity is assembled in a glove-box pressurised with purified nitrogen gas. At room temperature the pressure in the cavity is of the order of 10^{-5} Torr and the electroplated surfaces were not subjected to additional annealing processes.

2.1.2. Bulk $In_{.92}Pb_{.08}$- alloy test piece

The choice of the indium-lead alloy for this study was prompted by the fact that the metallurgy, critical temperature, critical fields and other superconducting properties, had been thoroughly investigated by Noto et al.[8] and Gygax[9].

Although an alloy containing lead less than 17 Wt o/o is considered as a solid solution[10], a study by Merriam[11] revealed an anomalous behaviour of this system in the superconducting transition temperature and the lattice parameter at about 11 to 14 Wt o/o Pb. On the other hand, only alloys with a concentration above about 7 Wt o/o Pb[8] show the second-kind superconductivity in the whole superconducting temperature range. Therefore, an alloy containing 8 Wt o/o Pb ($In_{.92}Pb_{.08}$) was employed in the present investigation.

The polycrystalline specimen, prepared from In and Pb of 99.99 o/o in purity, was supplied by Billiton, Arnhem, Holland. Diameter and thickness of the test pieces are respectively 137 mm and 7.6 mm. The surface was carefully machined, cleaned and dried, but no special heat treatment or surface polishing was carried out.

The $In_{.92}Pb_{.08}$-disk was attached to the copper bottom plate as shown in Fig. 1b. The thermal contact was made either by soldering (Wood's metal) the two pieces together or by applying a light mechanical pressure. As it will be shown later, further improvements are however necessary in order to reduce the temperature increase of the $In_{.92}Pb_{.08}$-surface during high power level measurements.

2.2. MEASUREMENT TECHNIQUES

The apparatus and experimental procedure adopted is similar to that described in a previous report[7] and only a brief description as well as some relevant relations will be given here.

Low temperature measurements are performed in a nested glass Dewar or stainless steel Dewar system, and temperatures between 4.2 K and 1.5 K can be obtained. Measurement of the temperature is made by observing the vapour pressure of the helium bath and checked by measuring the resistance of a previously calibrated carbon resistor which is attached to the cavity. The temperature is converted from the pressure using the "1958 scale of temperatures"[12]. A magnetic shield (μ-metal) immersed in the liquid helium bath, cancelled the earth's magnetic field to better than 5×10^{-3} Gauss.

During the measurements the cavity is suspended vertically by a thin walled stainless steel tube (Ø 120 mm), which serves also as the pumping line to evacuate the cavity through the coupling holes. The cavity is connected to the measuring devices by two inner stainless steel tubes whose walls (1) serve as the outer conductor of the coupling coaxial lines (50 ohms) and (2) terminate in a small loop penetrating through a cut-off tube in the upper end plate of the cavity (Fig. 1a). The coupling loops do not protude into the cavity, but can be withdrawn to adjust the coupling.

The surface resistance is experimentally determined by a measurement of the unloaded quality factor, Q_0 , of the cavity. In the geometry used (see Fig. 1a), the surface resistance is related to Q_0 by the geometrical factor : $R \cdot Q_0 = 780$ Ohms. The average surface resistance is given by :

$$R = 0.8565\, R_1 + 0.07196\, (R_2 + R_3) \qquad (1)$$

where R_1, R_2, R_3 are the surface resistances of the cylinder wall and the end plates, respectively.

The measured surface resistance ($R_{exp.}$) is equal to the sum of a temperature dependent term (R_T) which has to be fitted with the theoretical value, and a constant term which is the residual surface resistance ($R_{res.}$). In our TE_{011} mode cavities, with one end plate made of indium or indium-lead alloy, the temperature dependent surface resistance of these metals is given by

$$R_T(In;In_{.92}Pb_{.08}) = \frac{1}{0.072}[R_{exp.}(cav.) - R_{res.}(cav.) - 0.928 R_T(Pb)] \quad (2)$$

where $R_{exp.}(cav.)$ and $R_{res.}(cav.)$ are the measured and residual surface resistance of the whole cavity, and R_T (Pb) is the temperature dependent surface resistance of lead.

The loaded quality factor, Q_L, was measured with the decrement method using at high power a TWT-amplifier (1 W, 10 W or 300 W) driven by the cavity [7, 13]. At very low power levels ($\leq$ 15 mW) the measurement of Q_L was conveniently performed with the independent generator technique using a microwave signal generator Shlumberger Type FSO 1506. In order to avoid a coupling of the TE_{011} and TM_{111} modes, present in the cylinder geometry of the cavity, a mode-trap is installed in the bottom plate of the cavity (Fig. 1a).

The unloaded quality factor, Q_o, is determined from the relation $Q_o = Q_L(1 + \beta_1 + \beta_2)$ where β_1 and β_2 are the input and output coupling constants given by $\beta_1 = P_{rad}/P_c$ and $\beta_2 = P_t/P_c$ with P_{rad} = radiated power, P_c = power dissipated in the cavity and P_t = transmitted power. The power dissipated in the cavity is calculated from $P_c = P_i - P_r - P_t$ with P_i = incident power and P_r = the power reflected from the cavity.

These measurable quantities enable us to deduce the RF magnetic field on the cavity walls. In the case of our TE_{011} mode cavities, the peak RF magnetic fields, calculated from the field distribution [14] are given by :

$$B_{max} = 3.41 \times 10^{-3} (Q_o P_c)^{1/2} \quad \text{on the cylinder wall} \qquad (3)$$

and

$$B_{max} = 2.02 \times 10^{-3} (Q_o P_c)^{1/2} \quad \text{on the end plates} \qquad (4)$$

where B is in Gauss and P_c in Watt.

As can be seen, the maximum RF magnetic field on the bottom plate is lower by a factor of about 1.6 than at the centre of the lead covered cylindrical wall.

3. TEMPERATURE DEPENDENT MEASUREMENTS OF THE SURFACE RESISTANCE

3.1. EXPERIMENTAL RESULTS

The unloaded Q of TE_{011} mode cavities was measured at 293^oK, 77^oK and in the liquid helium temperature range. Typical values obtained are Q_o (293K) $\simeq 1.2 \times 10^4$ and Q_o (77K) $\simeq 3.6 \times 10^4$.

In the liquid helium temperature range a distinction has to be made between the indium layers obtained from the sulfate or fluoborate electroplating solutions. Curve (a) in Fig. 2 shows the Q_o-variation as a function of temperature for a representative cavity containing a bottom plate covered with indium from the sulfate solution. These data were taken at 2.85 GHz and at very low power levels. The critical temperature of the indium layer was about 3.3 K. This value has to be compared with the values reported in the literature, $T_c \simeq 3.4$ K[15)]. The Q_o-value at 4.2 K was of the order of 1.7×10^6, corresponding to a normal state surface resistance value for indium, R_N (4.2 K) = 6.4×10^{-3} Ohms.

For an indium layer from the fluoborate solution, Q_o(4.2 K) was of the same order of magnitude but the T_c-value was much lower, as can be seen in Fig. 2 (curve (b)). Without going into a detailed analysis of this low T_c-value, we can nevertheless refer to the presence of Ni and Fe in the electroplating fluoborate solution.

According to Reif et al.[16] the decrease of $T_c(dT_c)$ as a function of Fe concentration (c) in indium is given by $dT_c/d_c \simeq -2.0$ K/at o/o Fe. The measured T_c-decrease ($\simeq 0.9$ K) corresponds to approximately 0.195 Wt o/o Fe or Ni in the layer. The total amount of ferromagnetic material, compared with In, in the electroplating fluoborate solution is about 0.035 Wt o/o. This is still a factor of 5 too low to explain the observed T_c-decrease although it might well be that the Fe or Ni atoms are concentrated in a thin surface layer.

Except for a brief comment in Section 4.1.1, only the results obtained on indium layers from the sulfate solution will be analysed.

The temperature dependence of Q_o, measured at 2.85 GHz, for a representative TE_{011} mode electroplated lead cavity is illustrated in Fig. 5. The unloaded Q rises from $\simeq 2.3 \times 10^8$ at 4.2 K to $\simeq 8 \times 10^9$ at 1.5 K. The residual Q_o-value, $\simeq 8.3 \times 10^9$, is reproducible and comparable with the values measured in other laboratories[17]. This reproducibility is however only achieved by a careful treatment of the cavity before, during and after the plating process. Moreover, it seemed that ageing of the plating bath (2-3 weeks) may substantially decrease the $Q_{res.}$-values. The critical temperature of the lead layers has not been measured but may reasonably be assumed to be equal to the value reported in the literature (T_c(Pb) = 7.2 K).

Fig. 3 shows the Q_o-data, measured at 2.85 GHz, as a function of temperature for a TE_{011} mode cavity containing an $In_{.92}Pb_{.08}$-disc. The Q_o-values at 4.2 K and 1.5 K are respectively 6×10^5 and 1.13×10^9. It follows that the normal state low temperature surface resistance of the $In_{.92}Pb_{.08}$ specimen, $R_N(4.2\ K) = 1.8 \times 10^{-2}$ Ohms, is about three times higher than the value obtained for the indium layer. This corresponds to a pronounced decrease of the electron mean free path in the indium-lead alloy sample (See Section 3.2.3.).

The transition temperature of the sample, $T_c = 3.71$ K, is in remarkable agreement with the value derived from experimental data reported by Noto et al.[8] and Gygax[9]. This indicates that even in a thin surface layer of our $In_{.92}Pb_{.08}$ sample, the concentration homogeneity is comparable with the bulk of the material.

3.2. COMPARISON BETWEEN EXPERIMENT AND THEORY

3.2.1. Electroplated indium

The temperature dependent term of the superconducting surface resistance at a fixed frequency, $f = \omega/2\pi = 2.85$ GHz, is a function of several parameters. They are, the electron mean free path, ℓ ; the Fermi-velocity, v_F ; the London penetration depth, λ_L ; the critical temperature, T_c, and the energy gap 2Δ. The first three electronic parameters can be calculated from low temperature normal-state measurements of the surface resistance and the electronic specific heat.

The behaviour of metals at low temperatures and microwave frequencies is described by Reuter and Sondheimer's[18] theory of the anomalous skin effect. This behaviour is charaterized by a dimensionless parameter α , which may be expressed as

$$\alpha = \frac{3}{4}\, \mu_o \omega \left(\frac{1}{\rho\ell}\right) (\ell^3)$$

where μ_o is the permeability of the metal and ρ is the normal state DC electrical resistivity. According to the results published by Chambers[19], the classical condition holds for $\alpha \leq 0.016$. In this case, the surface resistance is given by

$$R_c = \left[\frac{1}{2}\, \mu_o \omega (\rho\ell) \left(\frac{1}{\ell}\right) \right]^{1/2} \quad (5)$$

In the region $\alpha \geqslant 3$ the surface resistance for a mean free path ℓ is adequately expressed by the following interpolation formula

$$R_\ell = R_\infty (1 + 1.157\ \alpha^{-0.2757}) \qquad (6)$$

where R_∞ is the surface resistance in the extreme anomalous region $(\alpha \rightarrow \infty)$:

$$R_\infty = \left[\sqrt{3}\pi \left(\frac{\mu_0}{4\pi}\right)^2\right]^{\frac{1}{3}} \omega^{\frac{2}{3}} (\rho\ell)^{\frac{1}{3}} = 3.789\times10^{-5} [\omega^{\frac{2}{3}} (\rho\ell)^{\frac{1}{3}}] \qquad (7)$$

Relations (6) and (7) are only valid for diffuse reflection of the conduction electrons at the metal surface. In the case of electroplated (In and Pb) or machined $(In_{.92}Pb_{.08})$ surfaces this assumption is justified since specular reflection has only been observed for very smooth and pure surfaces.

With eqs (6) and (7) we are able to calculate the mean free path ℓ if the $\rho\ell$-value is known. Although $\rho\ell$ is a constant, typical for each metal and independent of either purity or temperature, several experimental values, differing by as much as a factor of 4 , have been reported for indium[20, 21].

In order to bring the theoretical superconducting surface resistance of indium into better agreement with the measured data, the value of $\rho\ell = 0.89\times10^{-11}$ Ohms $\cdot$ cm^2 obtained by Roberts[22] from anomalous skin effect measurements was choosen. With this $\rho\ell$-value and the measured normal state surface resistance for In, $R_N(4.2K) = R_\ell(4.2K) = 6.4\times10^{-3}$ Ohms, the mean free path of the indium samples is of the order of 2.5×10^{-5} cm. (The values reported by Turneaure[1]) for electroplated Pb and Sn are respectively $\ell_{4.2K}(Pb) \simeq 7\times10^{-5}$ cm and $\ell_{4.2K}(Sn) \simeq 3.5\times10^{-5}$ cm or 8×10^{-5} cm).

The Fermi velocity, v_F, and the London penetration depth at 0K , $\lambda_L(0)$, can be related to the normal state free electron parameters in the following way[23, 24] :

$$v_F = \left(\frac{\pi^2 K^2}{e^2}\right)\left(\frac{1}{\gamma\rho\ell}\right) \qquad (8)$$

and

$$\lambda_L(0) = \left(\frac{e}{k\pi\sqrt{\mu_0}}\right)\left(\rho\ell\sqrt{\gamma}\right) \qquad (9)$$

with K the Boltzmann constant, e the electronic charge and γ the coefficient of electronic specific heat in the normal state.

If we substitute into eqs. (8) and (9) $\rho\ell$ = 0.89×10^{-11} Ohms·cm^2 and $\gamma = 1.7\times10^{-3}$ J/mole·deg^2 [25], which is the average of caloremetric values reported by Clement et al.[26] and Bryant et al.[27], we obtain v_F = 7.44×10^7 cm/s and $\lambda_L(0) = 3.1\times10^{-6}$ cm. The value for v_F is in good agreement with the value reported by Markowitz et al.[28], $v_F = 7.2\times10^7$ cm/s. The $\lambda_L(0)$-value has to be compared with the values reported respectively by Dheer[20], $\lambda_L(0) = 2.05\times10^{-6}$ cm, Fossheim[29], $\lambda_L(0) = 2.5\times10^{-6}$ cm, and Toxen[30], $\lambda_L(0) = 3.5\times10^{-6}$ cm.

The expression for the coherence length , ξ_0 , given by the B.C.S. theory[31] is :

$$\xi_0 = \hbar v_F / \pi\Delta(0) \qquad (10)$$

If we substitute into eq. (10) , $v_F = 7.44\times10^7$ cm/s and $\Delta(0) = 1.75\ KT_c$, we obtain $\xi_0 = 3.14\times10^{-5}$ cm. This value seems reasonable if compared with the data reported by Dheer[20], $\xi_0 = 4.4\times10^{-5}$ cm, Fossheim[29] , $\xi_0 = 2.0\times10^{-5}$ cm and Toxen[30], $\xi_0 = 2.6\times10^{-5}$ cm.

With these material parameters the superconducting surface resistance of indium has been calculated for diffuse reflection of the electrons at the surface using a computer program written by Halbritter[32].

Substituting into eq. (2) respectively $R_{res.}(cav.) = 5.6\times10^{-7}$ Ohms and the $R_T(Pb)$-values measured in a lead plated TE_{011}-mode cavity (see Section 3.2.2) we are able to calculate $R_T(In)$ from the measured $R_{exp.}(cav.)$ values.

As shown in Fig. 4, where $R_T(In)$ is plotted on a logarithmic scale as a function of T_c/T, the observed temperature dependence as well as the absolute values of the surface resistance at 2.85 GHz are in good agreement with the predictions of the microscopic theory.

3.2.2. Electroplated lead

In the case of lead, with a $T_c \approx 7.2$ K, the mean free path needed to calculate the surface resistance is less well defined, since the normal-state low temperature surface resistance could not be measured. Nevertheless, we were able to estimate ℓ by comparing the superconducting surface resistance measured at 4.2 K with the theoretical surface resistance calculated for different electron mean free path values. (At 4.2 K the residual surface resistance is negligible).

The best agreement was obtained for a value of the order of $\ell = 2\times10^{-5}$ cm. This value seems reasonable if compared with the crystal-size measurements performed by Salaün [33] on electroplated lead surfaces.

For comparison with the experimental results, the following parameters were used in the calculation of $R_T(Pb)$: London's penetration depth $\lambda L(0) = 2.8\times10^{-6}$ cm [34], coherence length $\xi_0 = 1.115\times10^{-5}$ cm [34], reduced energy gap at OK , $\Delta(0)/KT_c = 2.05$ [1, 35], critical temperature $T_c = 7.2$ K, electron mean free path $\ell = 2\times10^{-5}$ cm.

The dependence of the theoretical Q-value ($R.Q = 780$ Ohms) on temperature, calculated at 2.85 GHz for diffuse reflections of the electrons at the surface, is shown in Fig. 5 (dashed curve). The Q-variation as a function of temperature, derived from the theoretical values by taking into account the residual Q_0-value ($= 8.3\text{x}10^9$) is also plotted in Fig. 5 (full curve).

As can be seen, the agreement between the experimental data and the theory for our Pb-layers is good.

3.2.3. Indium-lead Alloy

In order to know how dirty the specimen is, the mean free path of the electrons is evaluated. Assuming that the $\rho \ell$-value for $In_{.92}Pb_{.08}$ is the same as for In ($\rho \ell = 0.89\text{x}10^{-11}$ Ohms$\cdot$cm^2), ℓ can be estimated from the measured value of the low-temperature normal-state surface resistance of $In_{.92}Pb_{.08}$, $R_N(4.2\text{ K}) = 1.8\text{x}10^{-3}$ Ohms. With this high $R_N(4.2\text{ K})$-value, the classical limit formula (eq. (5)) has to be used and gives a mean free path of the order of $2.5\text{x}10^{-6}$ cm.

This value seems reasonable if compared with $\ell \simeq 4.5\text{x}10^{-6}$ cm reported by Noto et al.[8] and Gygax[9] for well annealed and polished $In_{.92}Pb_{.08}$ samples.

The superconducting surface resistance of the In-Pb alloy has been calculated, for diffuse reflection of electrons at the surface, with the microscopic theory[32]. The parameters used in the numerical calculation are the same as for indium except the electron mean free path $\ell = 2.5\text{x}10^{-6}$ cm and the critical temperature $T_c = 3.71$ K.

Using the same procedure as for indium, but with $R_{res.}(\text{cav.}) = 2.6\text{x}10^{-7}$ Ohms, we can calculate the temperature dependent part of the measured surface resistance of the alloy. Values of $R_T(In_{.92}Pb_{.08})$, plotted on a logarithmic scale as a function of T_c/T, are shown in Fig. 6. The theory clearly reproduces correctly, within the experimental accuracy, the general form of variation of R_T $(In_{.92}Pb_{.08})$ with temperature. The agreement in absolute value is also satisfactory.

4. THE CRITICAL MAGNETIC FIELD

We do not want to repeat the complete discussion given by Turneaure[1] on the RF critical field measurements since the experimental problems as well as the observed phenomena are comparable.

Therefore, besides the experimental results, only a brief description of some interesting observations will be given. The high-power measurements on In and $In_{.92}Pb_{.08}$ were performed in lead-plated TE_{011} mode cavities with one end plate electroplated with indium or consisting of the indium-alloy disc. Since the DC as well as the RF critical magnetic field of Pb (see below) is much higher than that of In or the In-alloy, it is obvious that the measured data will be completely determined by the properties of these two metals.

4.1. HIGH LEVEL MEASUREMENTS AT 1.5 K

4.1.1. Electroplated Indium

The unloaded Q of a TE_{011}-mode cavity, measured at 1.5 K as a function of the power dissipated in the cavity P_c, is shown in Fig. 7.

Due to losses in the coupling system, the Q_o-values measured at low power levels are smaller than the value plotted in Fig. 2a at T = 1.5 K. Up to P_c-values of approximately 20 Watts, and within the experimental accuracy, no change in Q_o was observed. This indicates that the surface resistance is independent of the RF magnetic field for fields less than the critical field of In. At higher power levels, Q_o decreases abruptly by a factor of the order of 100 (approximately the normal state Q_o-value) and breakdown oscillations were observed, as illustrated in Photo 1, similar to those reported in a previous paper[6]. The magnetic field at which this instability occurs is called the RF critical magnetic field, B_c^{RF} .

The observed phenomena are due to a sudden change in the surface resistance, as a large portion of the indium becomes normal conducting. The corresponding maximum magnetic field on the In bottom plate, calculated with eq. (4) from the measured Q_o- and P_c-values is $B_c^{RF} = (225 \pm 10)$ Gauss. This value, measured at 1.5 K, is in good agreement with the DC critical magnetic field value, B_c (1.5 K) = 225 G, for bulk indium reported by Finnemore et al.[15].

The DC critical magnetic field of the indium layers was not measured but it seems reasonable to assume that this field corresponds with the value for bulk indium. (The measurements of Turneaure[1] on electroplated Sn-layers are consistent with this assumption).

The high power measurements were repeated over a period of one month without any notable change of the Q_o- or B_c^{RF}- values. During this period the cavity was always kept under a vacuum of about 10^{-5} Torr, but was repeatedly temperature-cycled between 4.2 K and 300 K.

Finally, it might also be interesting to mention the results obtained with indium from the fluoborate solution (T_c = 2.3 K). The peak RF magnetic field measured at 1.5 K was of the order of 90 Gauss. This value is about 50 o/o lower than the value calculated from the relation $B_c(T) = B_c(0)\ (1-(T/T_c)^2)$ with $B_c(0)$ = 282 G[15] and T_c = 2.3 K.

Although the experiment provides no information about the origin of this low B_c^{RF}-value, it is interesting to attempt a plausible explanation. If we assume that magnetic impurities are present in the In-layer, the use of the $B_c(0)$-value for pure In in order to calculate $B_c(T)$ is no longer justified. According to Maki[36] the decrease of the critical magnetic field in the extremely gapless region is given by $B_c(0) = B_{co}(0)\ (1- \alpha/\alpha_c)$. In this relation $B_{co}(0)$ is the critical field in the absence of impurities, $\alpha_c = \Delta_o(0)/2$

is the pair-breaking parameter in the extremely gapless region ($2\Delta_0/0$) = energy gap of pure metal) and α is the pair-breaking parameter related to the shift in T_c by the following expression, $T_c - T_{co} = -\pi/4\ \alpha$ · (T_{co} = transition temperature of pure metal). It follows that the critical field at 0K in the extremely gapless region is $B_c(0) \simeq 75$ G. The corresponding value at 1.5 K is of the order of 2 lower than the measured peak RF magnetic field. However, the impurity concentration in the In-layer is certainly lower than the critical concentration at which the superconductivity is completely quenched (extremely gapless region). It seems therefore quite plausible that the measured decrease of the RF critical magnetic field is due to the presence of magnetic impurities in the indium-layer from the fluoborate solution.

4.1.2. Electroplated lead

As shown in Fig. 8 , the Q_0-value at 1.5 K of a lead-plated TE_{011} mode cavity, measured as a function of P_c, decreased by approximately a factor of 2 . The observed decrease is however reversible and probably due to heating of the cavity walls which becomes important at power levels of the order of 120 Watts. At higher P_c-values, Q_0 decreases abruptly and breakdown oscillations were observed similar to those reported for indium. The corresponding peak RF magnetic field on the lead surface, calculated with eq. (3), is of the order of 750 Gauss. This B_c^{RF} value for lead is in good agreement with the DC critical field value at 1.5 K reported in the literature[37]. Although this critical RF field is, to our knowledge, the highest value obtained for lead, it is nevertheless still much lower than the superheating critical magnetic field. The same observation is also valid for the measured B_c^{RF}-values of indium (see Section 4.1.1.) and of tin[1].

4.1.3. Indium-lead Alloy

The unloaded Q of a lead-plated cavity containing an $In_{.92}Pb_{.08}$-disc, measured at 1.5 K as a function of P_c, is shown in Fig. 9. At P_c-values of about 0.8 Watt Q_0

decreased to a value which is still a factor of 20 higher than the normal state value. The corresponding maximum magnetic field on the In-alloy bottom plate is about 17 Gauss. This value is much less than the lower DC critical magnetic field B_{c1} for $In_{.92}Pb_{.08}$ which is 270 Gauss at 1.5 K[8]. However, the temperature increase of the sample surface is important due to the bad thermal contact between the He-bath and the sample, the thickness of the In-Pb alloy disc as well as the lower thermal conductivity of the alloy[38] if compared with pure indium. That heating effects are important and probably limited the B_{RF}-value for $In_{.92}Pb_{.08}$ could be verified by performing high power measurements as a function of pulse length. With microwave pulses of about 1.6 ms duration, which is the lowest value obtainable with the actual measuring circuit, magnetic breakdown was only observed at B_{RF}-values of the order of 90 Gauss.

The experimental difficulties may eventually be avoided by the use of a thin electroplated In-Pb alloy layer. Preliminary investigations indicated however that, besides problems with the electroplating bath, the homogeneity of the alloy is bad and difficult to control while the surface of the layer is irregular and probably oxidized.

Further improvements in the experimental set-up are thus necessary before a detailed study of B_{RF} as a function of material parameters, special metallurgical processes and temperature can be made.

4.2. HIGH LEVEL MEASUREMENTS AS A FUNCTION OF TEMPERATURE

In order to verify the temperature dependence of the RF critical magnetic field, measurements were made in the liquid helium temperature range on indium and lead electroplated TE_{011} mode cavities.

The temperature in this region was kept constant during a measurement by regulating the helium vapour pressure. The temperature stability of the helium bath, controlled with a carbon resistor, was better than 0.01^{o} K at low power level measurements. The duration of the microwave pulses was relatively short in order to prevent an excessive increase of the helium bath temperature and eventually boiling.

4.2.1. Electroplated indium

Due to the low thermal conductivity of He-I a distinction can be made between the measurements carried out below or above the -point of liquid helium (T_λ). The thermal conductivity of He-II is high and since the maximum RF power in the cavity is relatively low ($P_c$max $\simeq$ 20 Watts) it was not necessary to make a correction for the temperature data in this region. The Q-values were constant as a function of time (pulse length) which supports the view that the power dissipated on the cavity walls increased the temperature with a negligible amount.

The situation was more complicated above the transition point of liquid helium. The measurements were characterized by the following observations :

- at a temperature $T > T_\lambda$, the pulse-shape (Pt) was distorted as illustrated in Photo 2 ;
- a careful examination of the decay of the stored energy in the cavity indicated that Q_o changes in time (see photo 2 and ref. 6).

Both phenomena clearly indicate a no longer negligible temperature rise of the cavity walls and a temperature correction was necessary in this region. The temperature of the cavity surface was estimated using a method proposed by Turneaure[1]. The Q_o-value at high power levels, measured immediately after the incident power is removed, is compared with the Q_o-value measured at very low field levels. Since Q_o is approximately independent of the magnetic field until the critical field is reached, the temperature of the cavity surface can be estimated. Fig. 10 shows the experimental data for the RF critical magnetic field of indium as a function of temperature. The solid line is the DC critical magnetic field assuming that T_c equals the observed value (3.3 K) and $B_c(0)$ = 282 G.

The agreement between the RF and DC data is very good below the λ-point of liquid helium and near T_c, where the incident power is low.

The agreement is less satisfactory in the He-I region where rather high power levels are necessary and the estimation made of the indium surface temperature will be less accurate. Nevertheless, it seems to us that there are enough indications to conclude that the RF critical magnetic field of indium is consistent with the DC critical magnetic field. This observation is in agreement with Turneaure's[1)] results for tin and, as will be seen, is also valid for lead.

4.2.2. Electroplated Lead

Much higher power levels are needed, in the case of lead, in order to observe magnetic breakdown phenomena. Therefore, a temperature correction was also necessary in the He-II region. Measurements at very low power levels and with the same coupling loop position enabled us to take account of the temperature increase due to heating effects.

The maximum RF magnetic fields measured before the magnetic breakdown in a TE_{011} lead-plated cavity as a function of temperature are shown in Fig. 11.

The solid line is the DC critical magnetic field of bulk lead assuming that $T_c = 7.2$ K and $B_c(0) = 800$ Gauss[37)]. The correspondance between the RF and DC critical field data is satisfactory and indicates that also for lead both critical fields are consistent with each other.

5. CONCLUSIONS

Measurements on superconducting S-band TE_{011} mode cavities made of indium - and lead - plated copper or containing an indium-lead alloy disc have demonstrated that :

1) The measured microwave surface resistance of a type I superconductor (In and Pb) or a type II superconductor ($In_{.92}Pb_{.08}$) is in good agreement with the predictions of the microscopic theory.

2) The surface resistance of In and Pb is independent of the RF magnetic field, if heating effects are taken into account, up to a magnetic field value which is comparable with the DC critical magnetic field.

3) The same independency has been found for $In_{.92}Pb_{.08}$ up to a RF magnetic field level of about 17 G . This low B_{RF} value for the indium-alloy is due to heating effects as indicated by high power measurements as a function of pulse length. The maximum RF magnetic field, measured with the shortest pulse length, was about 90 G, which is still a factor 3 smaller than the lower DC critical magnetic field, $B_{c1} \approx 270$ G.

4) The RF critical magnetic field B_c^{RF}, of In and Pb as a function of temperature is adequately described by the thermodynamic theory of the DC critical field.

5) Exceeding the critical B_{RF} value of In and Pb results in an abrupt increase of the surface resistance up to the low temperature normal state value. This transition is characterized by magnetic breakdown and oscillation phenomena.

ACKNOWLEDGEMENTS

The authors thank Dr. Claude Germain for his interest in this work. We also wish to express our thanks to H. Rieder and U. Silvestri for their technical help during the measurements and to J.C. Dubois, W. Burkhalter and the personnel of the Atelier Godet for their assistance.

REFERENCES

1) TURNEAURE, J.P.,
Stanford University, HEPL Report No. 507 (1967)

2) TURNEAURE, J.P. and WEISSMAN, I.,
J. Appl. Physics 39 (1968) 4417

3) MATTIS, D.C. and BARDEEN, J.,
Phys. Rev. 111 (1958) 412 ;
ABRIKOSOV, A.A., GOR'KOV, L.P. and KHALATNIKOV, I.M.,
Soviet Physics - JETP 8 (1959) 182; 10 (1960) 132

4) HALBRITTER, J.,
KFZ- Karlsruhe, Externer Bericht 3/69-2 (1969)

5) GORLE, D., LEROY, D., MORIGNOT, P., RIEDER, H.
and BRUYNSERAEDE, Y.,
CERN/MPS/MU-NOTE SD 69-1 (1969)

6) GORLE, D., LEROY, D., MORIGNOT, P., RIEDER, H.
and BRUYNSERAEDE, Y.,
CERN/MPS/MU-SD 69-3 (1969)

7) GORLE, D., LEROY, D. and MORIGNOT, P.,
CERN/NPA/Int. 67-23 (1967)

8) NOTO, K., MUTO, Y. and FUKUROI, T.,
J. Physical Soc. Japan, 21 (1966) 2122

9) GYGAX, S.,
Phys. Kondens. Materie 4 (1965) 207

10) HANSEN, M.,
Constitution of Binary Alloys
(McGraw-Hill Book Company, Inc. 1958) 854

11) MERRIAM, M.F.,
Rev. Mod. Phys. 36 (1964) 152

12) BRICKWEDDE, F.G., VAN DIJK, H., DURIEUX, M.,
CLEMENT, J. and LOGAN, J.K.,
J. Res. Natl. Bur. Std. (U.S.A.) -
A Physics and Chemistry 64 (1960) 1.

13) GORLE, D., LEROY, D. and MORIGNOT, P.
CERN/MPS-MU/SD 70-1 (1970).

14) MONTGOMERY, C.G.,
Technique of Microwave Measurements, Vol. 11,
M.I.T. Radiation Lab. Series,
McGraw-Hill Book Company, Inc., N.Y. 1947.

15) FINNEMORE, D.K. and MAPOTHER, D.E.,
Phys. Rev. 140 (1965) 507

16) REIF, F. and WOOLF, M.A.,
Phys. Rev. Letters. 9 (1962) 315

17) SCHWETTMAN, H.A., WILSON, P.B., PIERCE, J.M. and FAIRBANK, W.M.,
Int. Advances in Cryogenic Engineering,
ed. Timmerhaus, K.D. (Plenum Press, N.Y. 1965) 10, 88;
HIETSCHOLD, R., LIST, R. and STOLTZ, O.,
KFZ- Karlsruhe, KFK-Bericht 872 (1968);
HAHN, H., HALAMA, H.J. and FOSTER, E.H.,
J. Appl. Phys. 39 (1968) 2606;
BENDALL, R.G., BRADY, B.G. and MILNE, J.D.,
Rutherford Lab., Nimrod (BP) 22 (1969).

18) REUTER, G.E.H. and SONDHEIMER, E.H.,
Proc. Roy. Soc. (London) A 195 (1948) 336

19) CHAMBERS, R.G.,
Proc. Roy. Soc. (London) A 215 (1952) 481.

20) DHEER, P.N.
Proc. Roy. Soc. (London) A 260 (1961) 333

21) TOXEN, A.M.,
Phys. Rev. 123 (1961) 442

22) See FABER, T.E.,
Proc. Roy. Soc. (London) A 241 (1957) 531

23) ZIMAN, J.M.,
Electrons and Phonons (Oxford Univ. Press., N.Y. 1960)

24) FABER, T.E. and PIPPARD, A.B.,
Proc. Roy. Soc. (London) A 231 (1955) 336.

25) The molar volume of In at 4 K is $V = 15.37\ cm^3/mole$;
SWENSON, C.A.,
Phys. Rev. 100 (1955) 1607

26) CLEMENT, J.R. and QUINNELL, E.H.,
Phys. Rev. 92 (1953) 258

27) BRYANT, C.A. and KEESOM, P.H.,
Phys. Rev. Letters 4 (1960) 460.

28) MARKOWITZ, C. and KADANOFF, L.P.,
Phys. Rev. 131 (1963) 563

29) FOSSHEIM, K.,
Phys. Rev. Letters 19 (1967) 81

30) TOXEN, A.M.,
Phys. Rev. 127 (1962) 382.

31) BARDEEN, J. COOPER, L.N. and SCHRIEFFER, J.R.,
Phys. Rev. 108 (1957) 1175

32) HALBRITTER, J.
KFZ- Karlsruhe, Externer Bericht 3/70-6 (1970)

33) SALAÜN, M.,
Thesis, Faculté des Sciences d'Orsay,
Institut d'Electronique Fondamentale (1969)

34) SMITH, F.W. and CARDONA, M.,
Sol. State Comm. 6 (1968) 37;
HALBRITTER, J.,
KFZ-Karlsruhe (to be published)

35) GINSBERG, D.M. and LESLIE, J.D.,
IBMJ. 6 (1962) 55

36) MAKI, K.,
Superconductivity, ed. Parks, R.D.
(Marcel Inc., N.Y. 1969) 1050

37) SEKULA, S.T. and KERNOHAN, R.H.,
J. Phys. Chem. Solids 27 (1966) 1863

38) FOX, G.T., WOLFMEYER, M.W. and DILLINGER, J.R.,
Phys. Rev. 177 (1969) 756;
MAMIYA, T.,
J. Phys. Soc. Japan 21 (1966) 1032

FIGURE CAPTIONS

Fig. 1 Cross-sectional view of (a) a TE_{011} mode cavity (dimensions in mm) showing the coupling system and mode trap, (b) the lower part of the cavity with an In-Pb alloy bottom plate.

Fig. 2 The temperature dependence of Q_o at 2.85 GHz for a Pb-plated TE_{011} mode cavity containing a bottom plate covered with In from the (a) sulfate solution, (b) fluoborate solution.

Fig. 3 The unloaded Q at 2.85 GHz as a function of temperature for a TE_{011} mode Pb-plated cavity containing an $In_{.92}Pb_{.08}$ disc.

Fig. 4 The measured and theoretical surface resistance of In at 2.85 GHz as a function of reduced temperature.

Fig 5 The Q_o-variation at 2.85 GHz as a function of temperature for a Pb-plated TE_{011} cavity. (x) = measured values; dashed curve = Q_o(theory); full curve = Q_o(theory- Q_o(residual).

Fig. 6 The measured and theoretical surface resistance of $In_{.92}Pb_{.08}$ at 2.85 GHz as a function of reduced temperature.

Fig. 7 Q_o as a function of P_c, and the corresponding peak surface RF magnetic fields on the In-layer measured at 1.5 K.

Fig. 8 Q_o as a function of P_c, and the corresponding peak surface RF magnetic fields for a lead plated TE_{011} mode cavity at 1.5 K.

<u>Fig. 9</u> Q_o as a function of P_c, and the corresponding peak surface RF magnetic fields on the In-alloy disc measured at 1.5 K.

<u>Fig. 10</u> The temperature dependence of the RF critical magnetic field of In measured at 2.85 GHz.

<u>Fig. 11</u> The RF critical magnetic field of Pb at 2.85 GHz as a function of temperature.

<u>Photo 1</u> Typical pulse shape (Pt) during breakdown oscillations. The horizontal scale is 0.1 s/div.

<u>Photo 2</u> Typical Q-variation as a function of pulse length. Short pulse $Q_o = 9.4\text{x}10^7$; Long pulse $Q_o = 6.9\text{x}10^7$. The horizontal scale is 0.05 s/div.

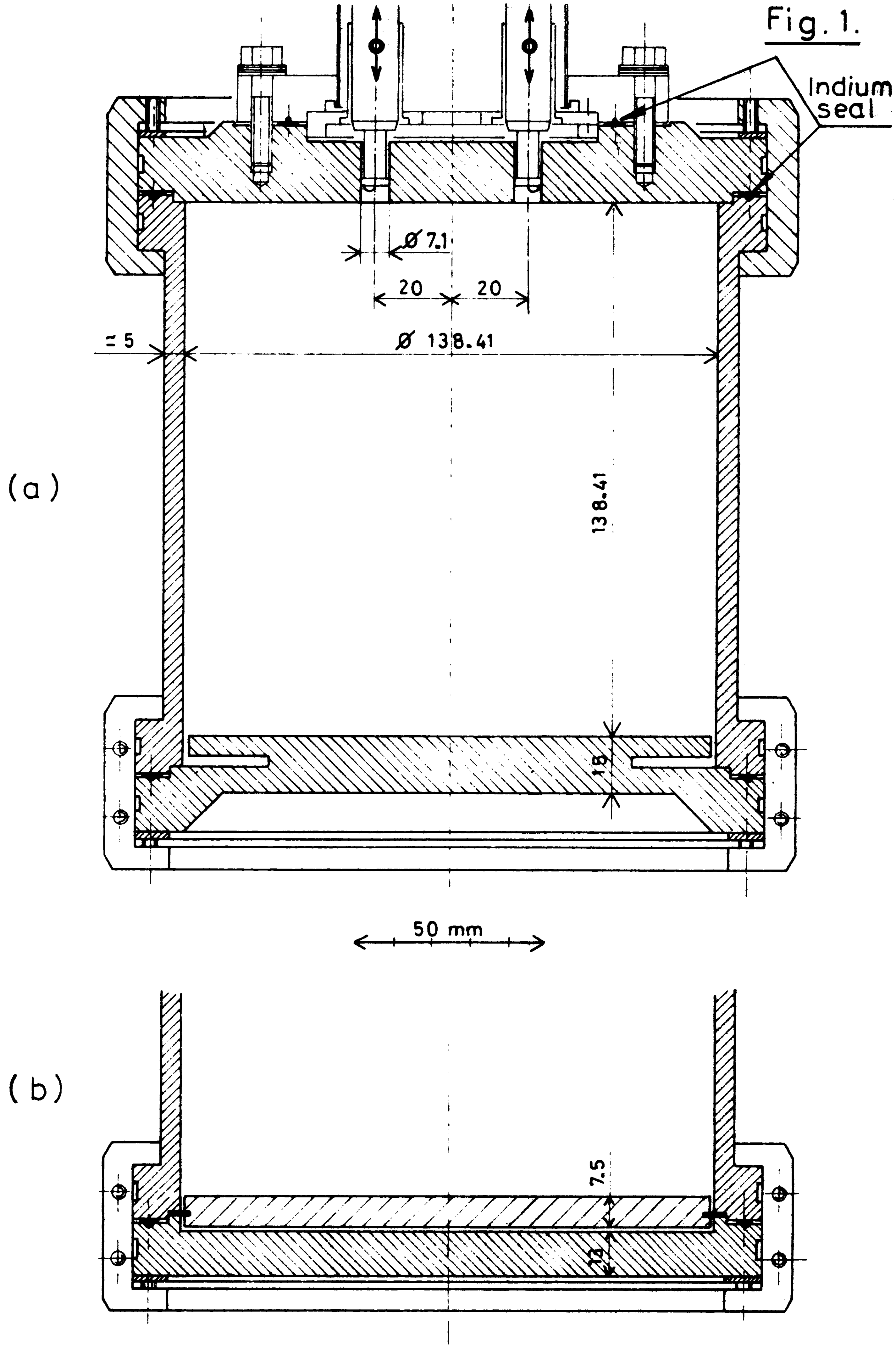
Fig. 1.
Indium seal
Ø 7.1
20
20
≈ 5
Ø 138.41
(a)
138.41
18
50 mm
(b)
7.5
13

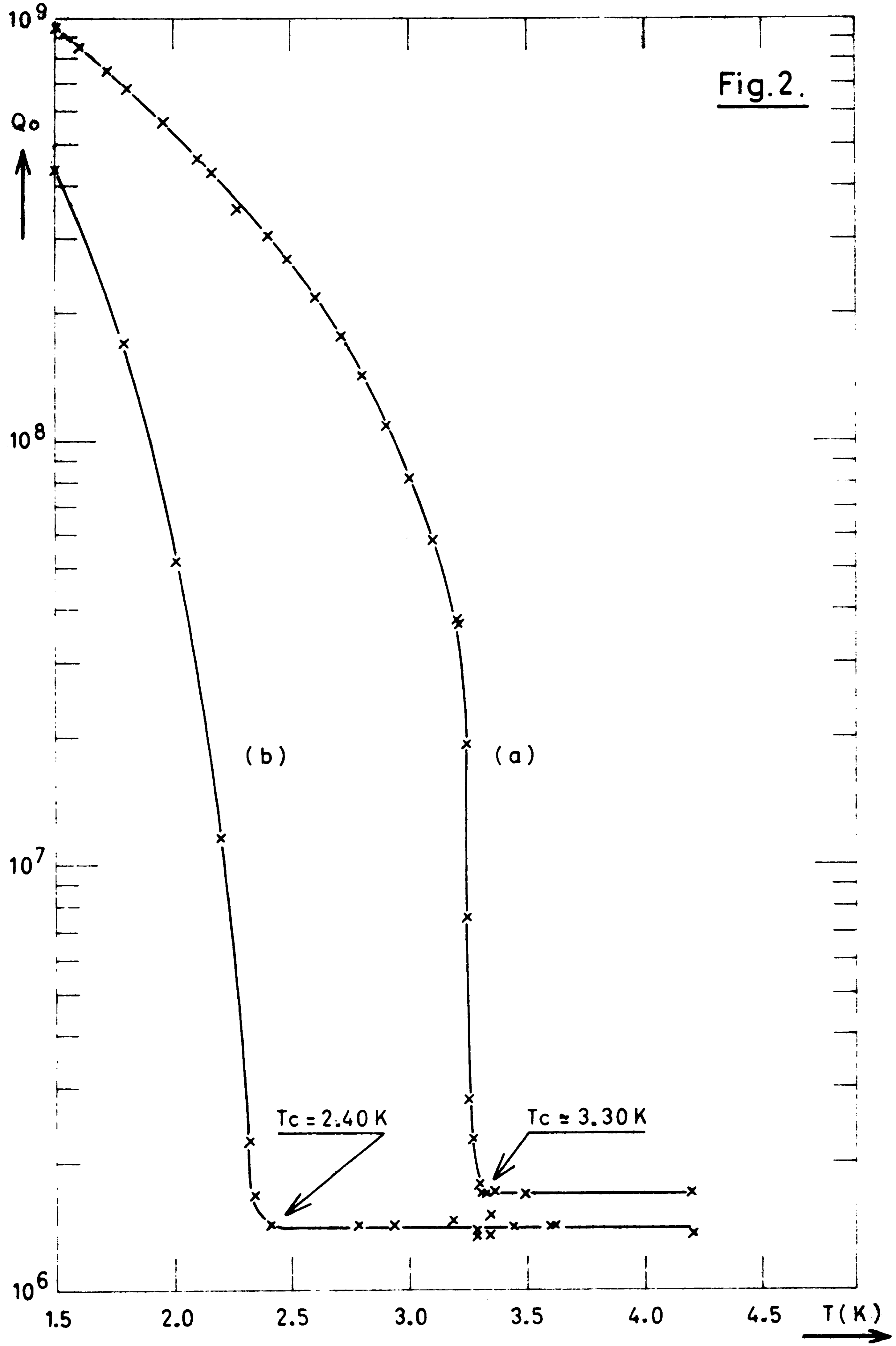
Fig. 2.
Qo
10^9
10^8
10^7
10^6
(b)
(a)
Tc = 2.40 K
Tc ≃ 3.30 K
1.5
2.0
2.5
3.0
3.5
4.0
4.5
T(K)

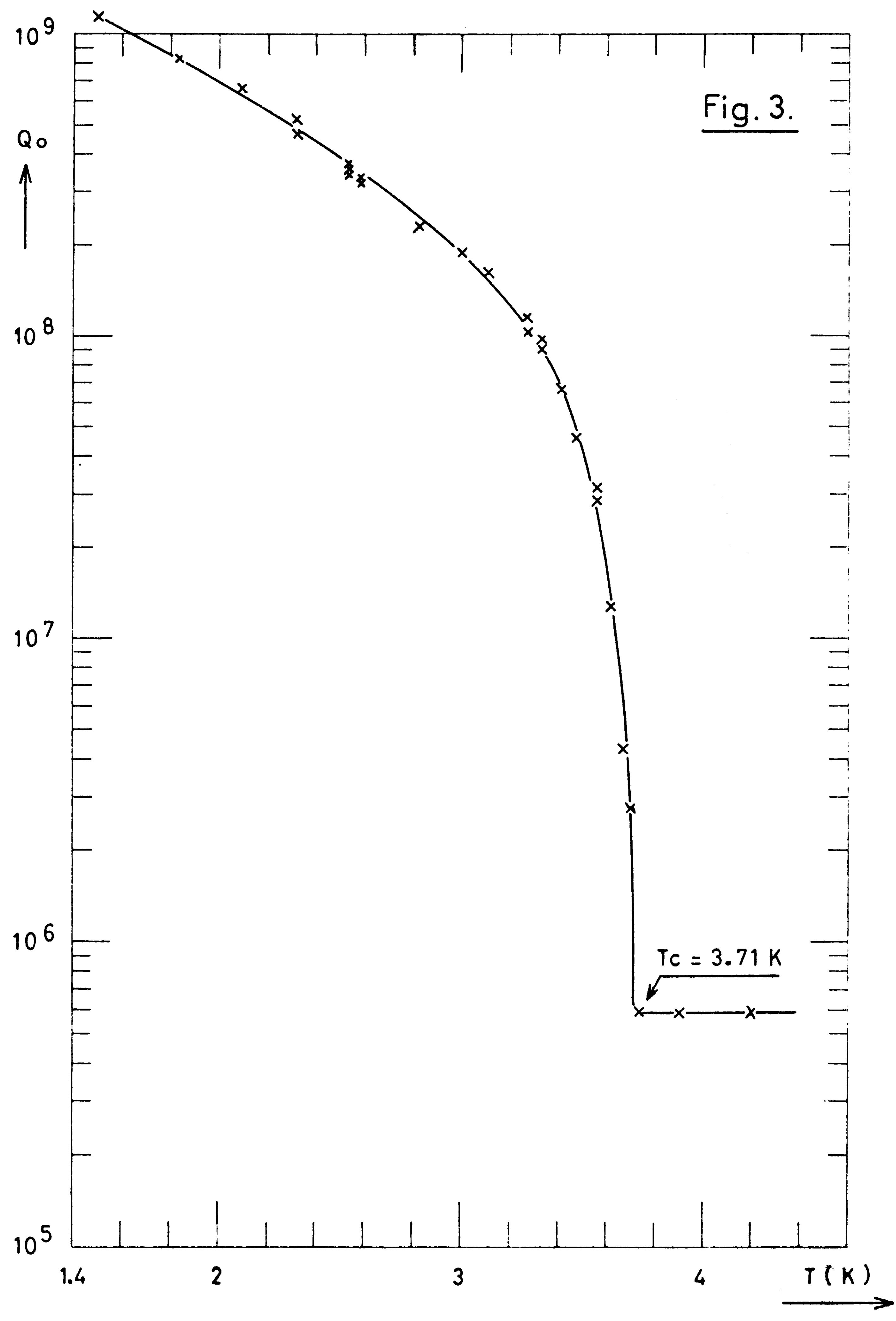

Fig. 3.
10^9
10^8
10^7
10^6
10^5
Q_o
Tc = 3.71 K
1.4
2
3
4
T (K)

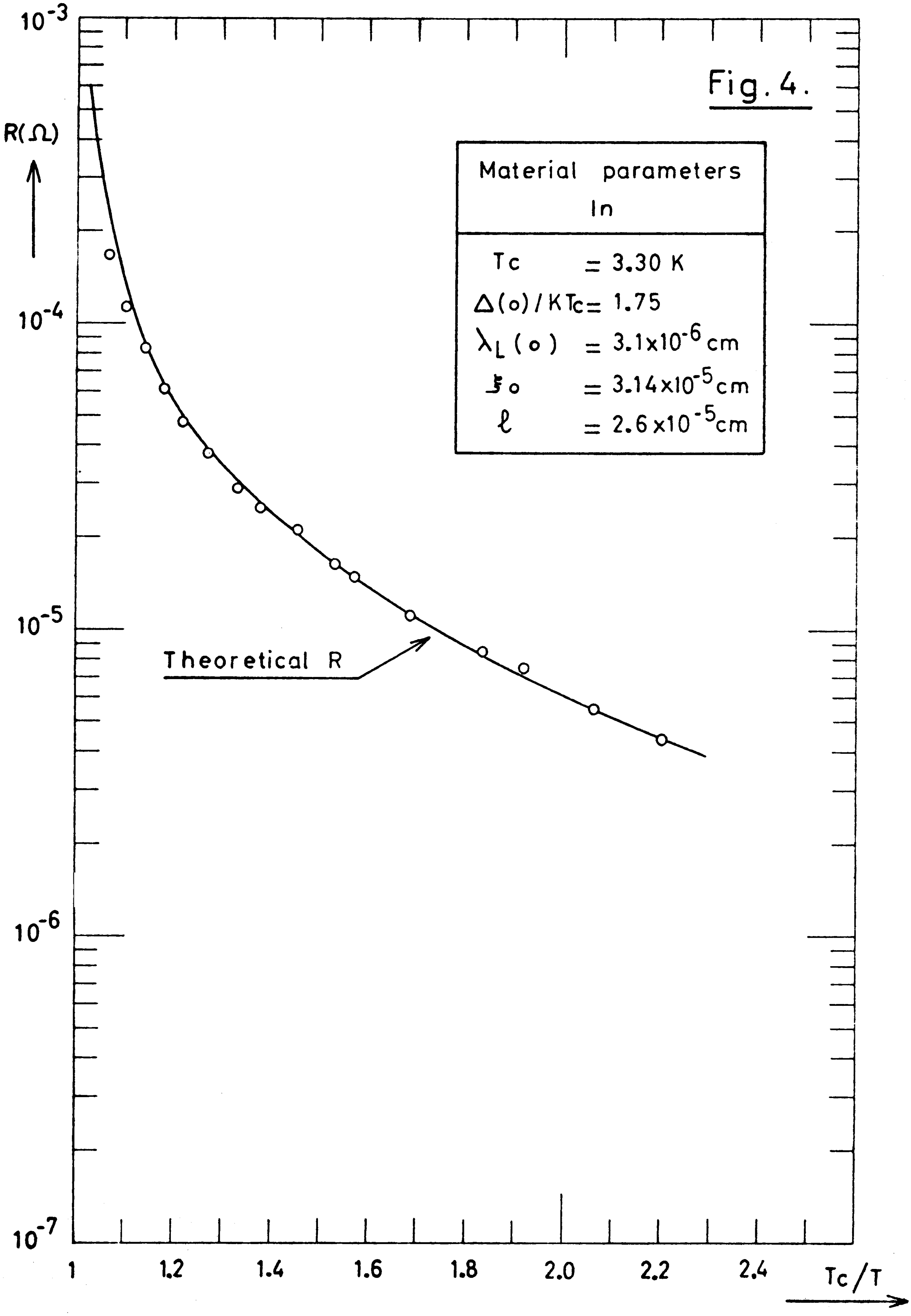
Fig. 4.
R(Ω)
Material parameters
In
Tc = 3.30 K
Δ(o)/KTc = 1.75
λL(o) = 3.1x10-6 cm
ξo = 3.14x10-5 cm
ℓ = 2.6x10-5 cm
Theoretical R
10-3
10-4
10-5
10-6
10-7
1
1.2
1.4
1.6
1.8
2.0
2.2
2.4
Tc/T

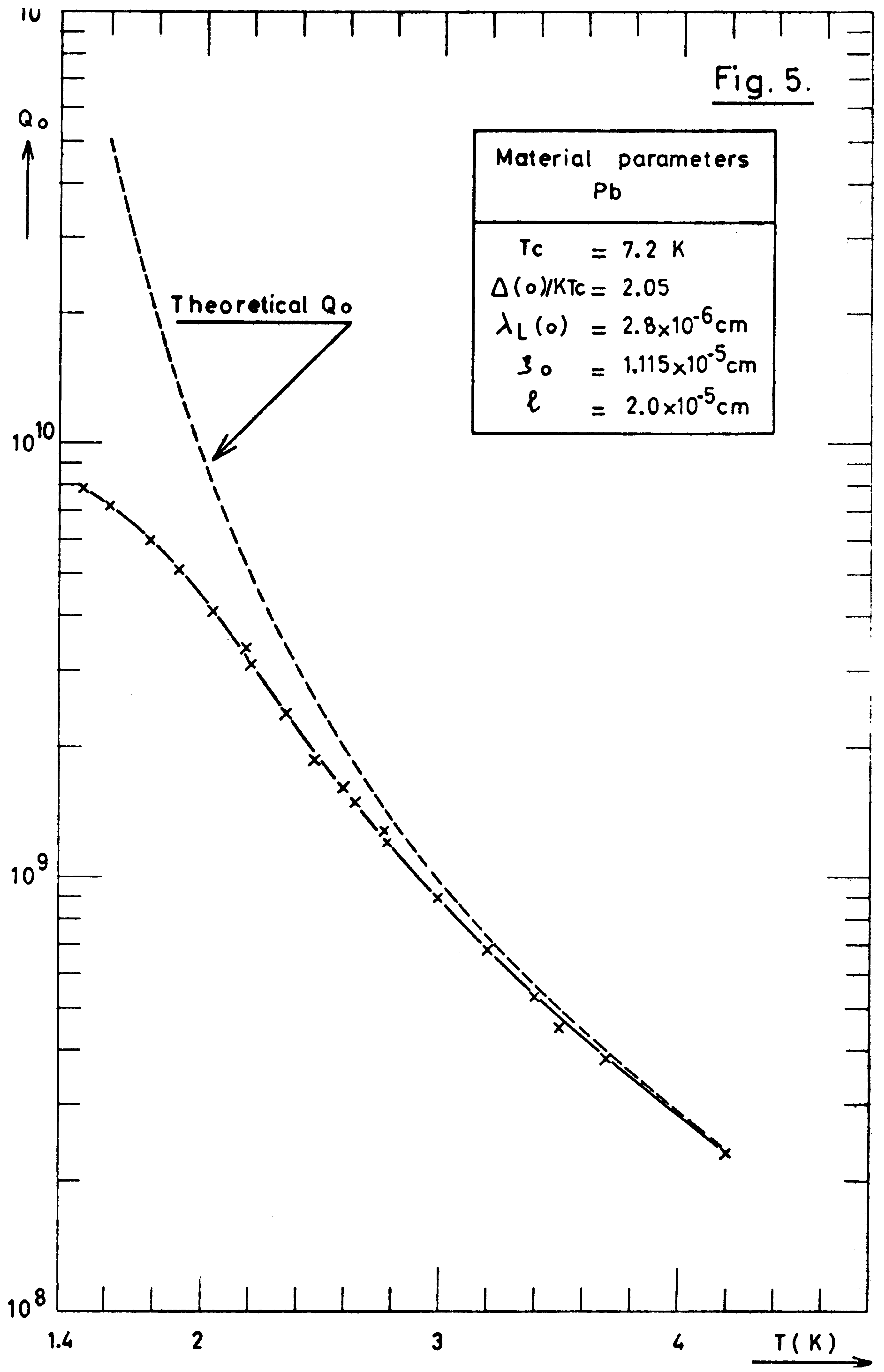

Fig. 5.
Material parameters
Pb
Tc = 7.2 K
Δ(o)/KTc = 2.05
λL(o) = 2.8x10^-6 cm
ξo = 1.115x10^-5 cm
ℓ = 2.0x10^-5 cm
Theoretical Qo
Qo
10^10
10^9
10^8
1.4
2
3
4
T(K)

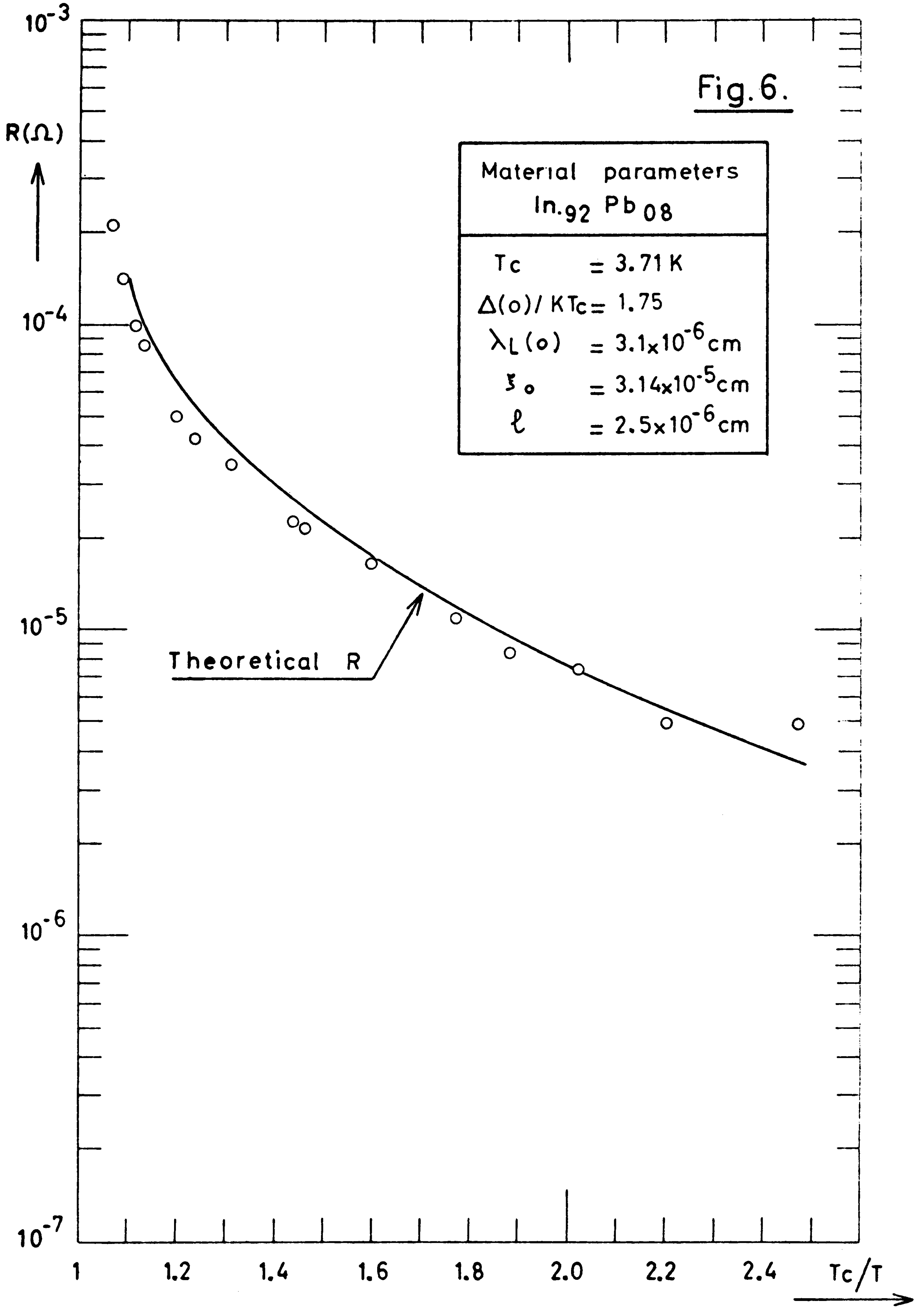

Fig. 6.
R(Ω)
10^-3
10^-4
10^-5
10^-6
10^-7
Material parameters
In.92 Pb 08
Tc = 3.71 K
Δ(o)/ KTc = 1.75
λL (o) = 3.1x10^-6 cm
ξo = 3.14x10^-5 cm
ℓ = 2.5x10^-6 cm
Theoretical R
1
1.2
1.4
1.6
1.8
2.0
2.2
2.4
Tc/T

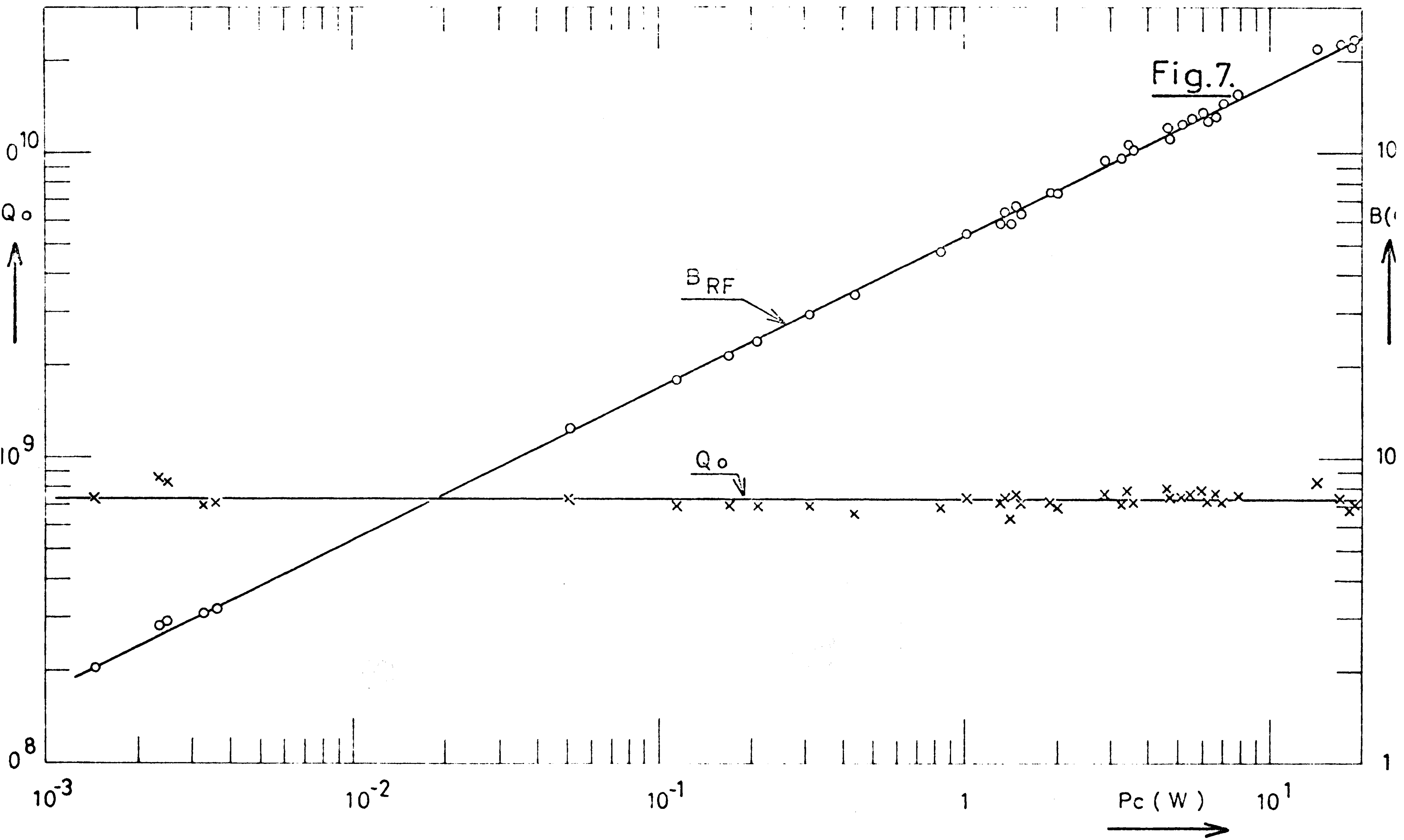

Fig.7.
B RF
Q o
Q o
B(
Pc (W)
10^-3
10^-2
10^-1
1
10^1
10^8
10^9
10^10
1
10
10

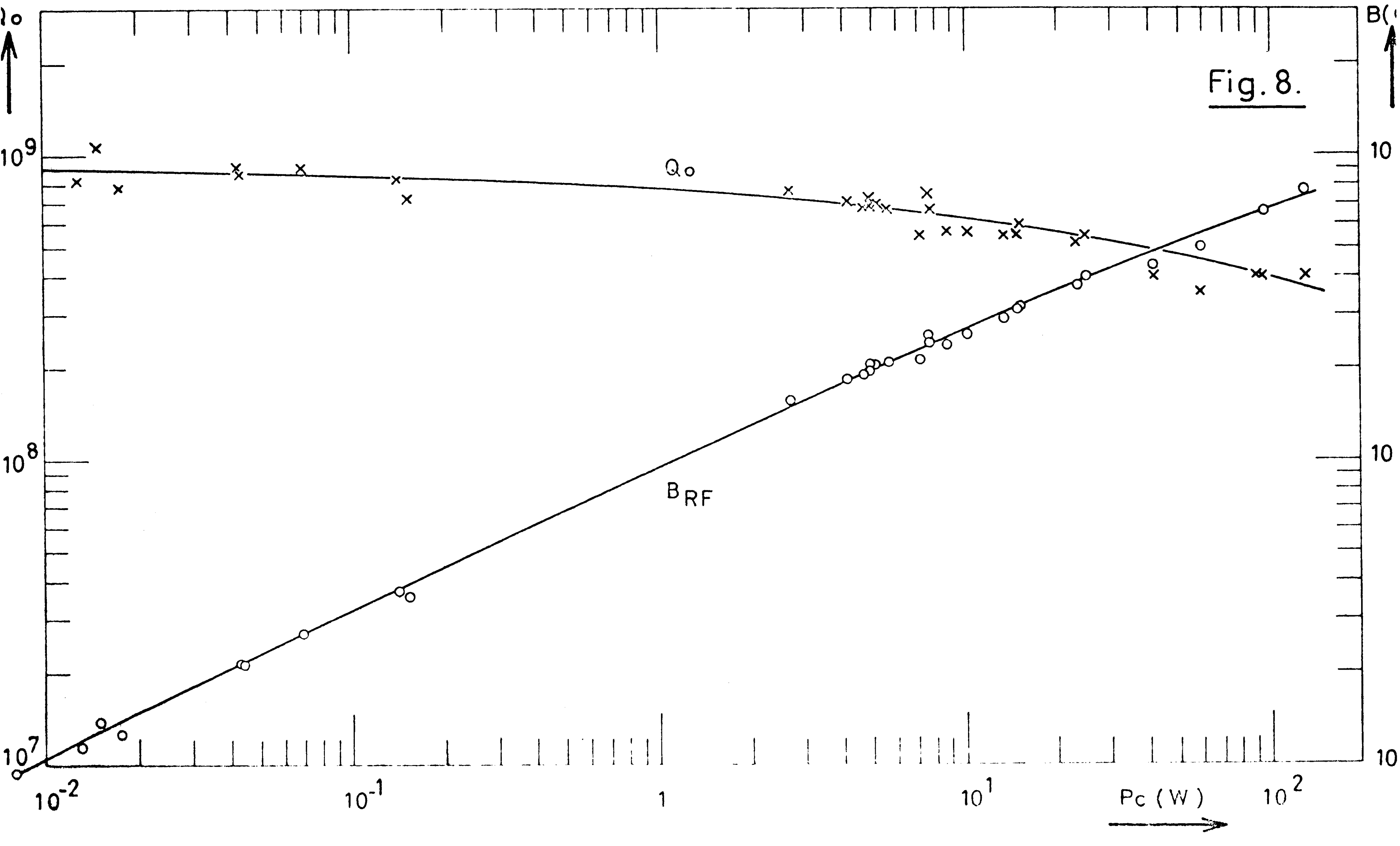

Fig. 8.

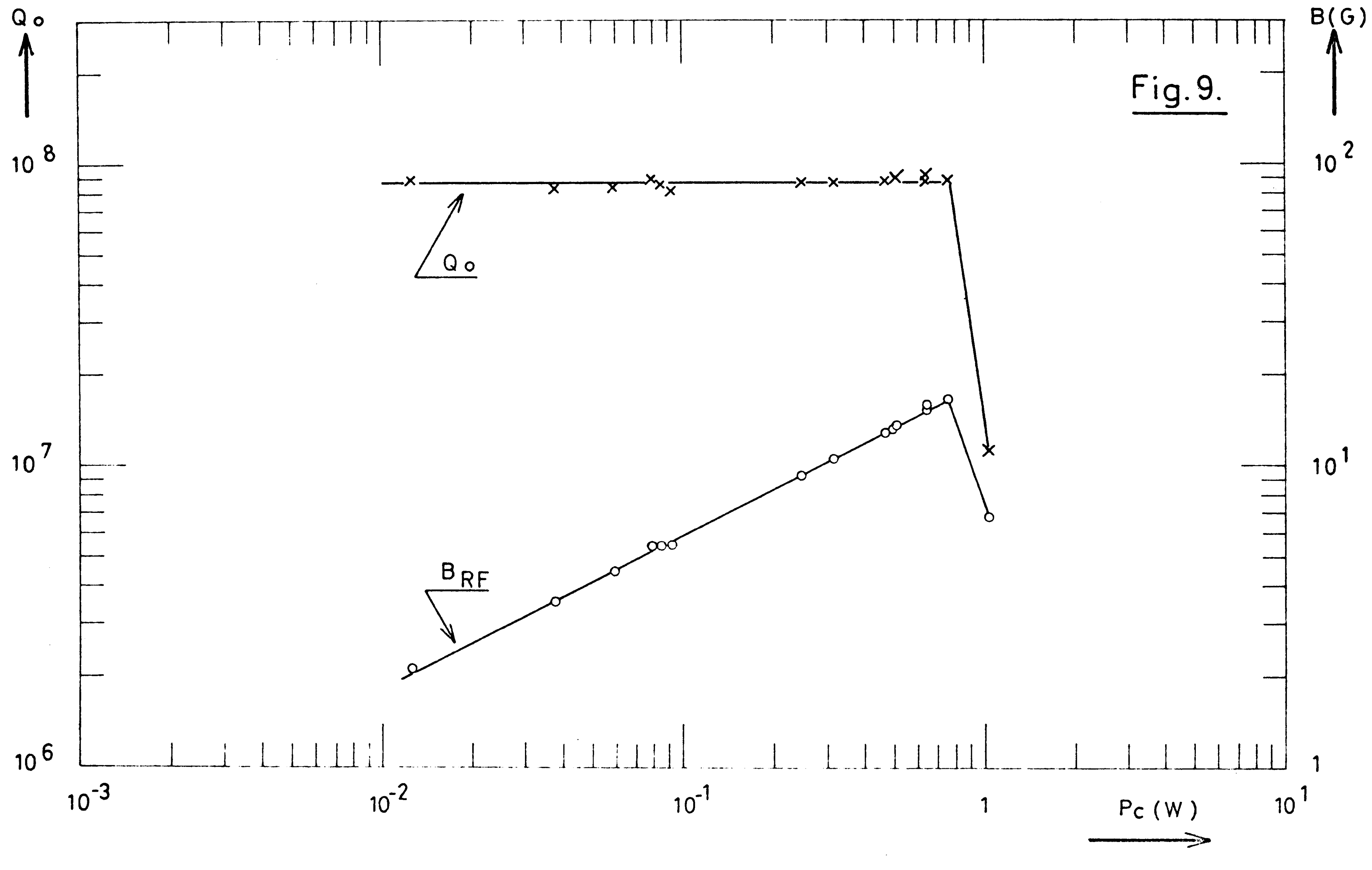

Fig. 9.

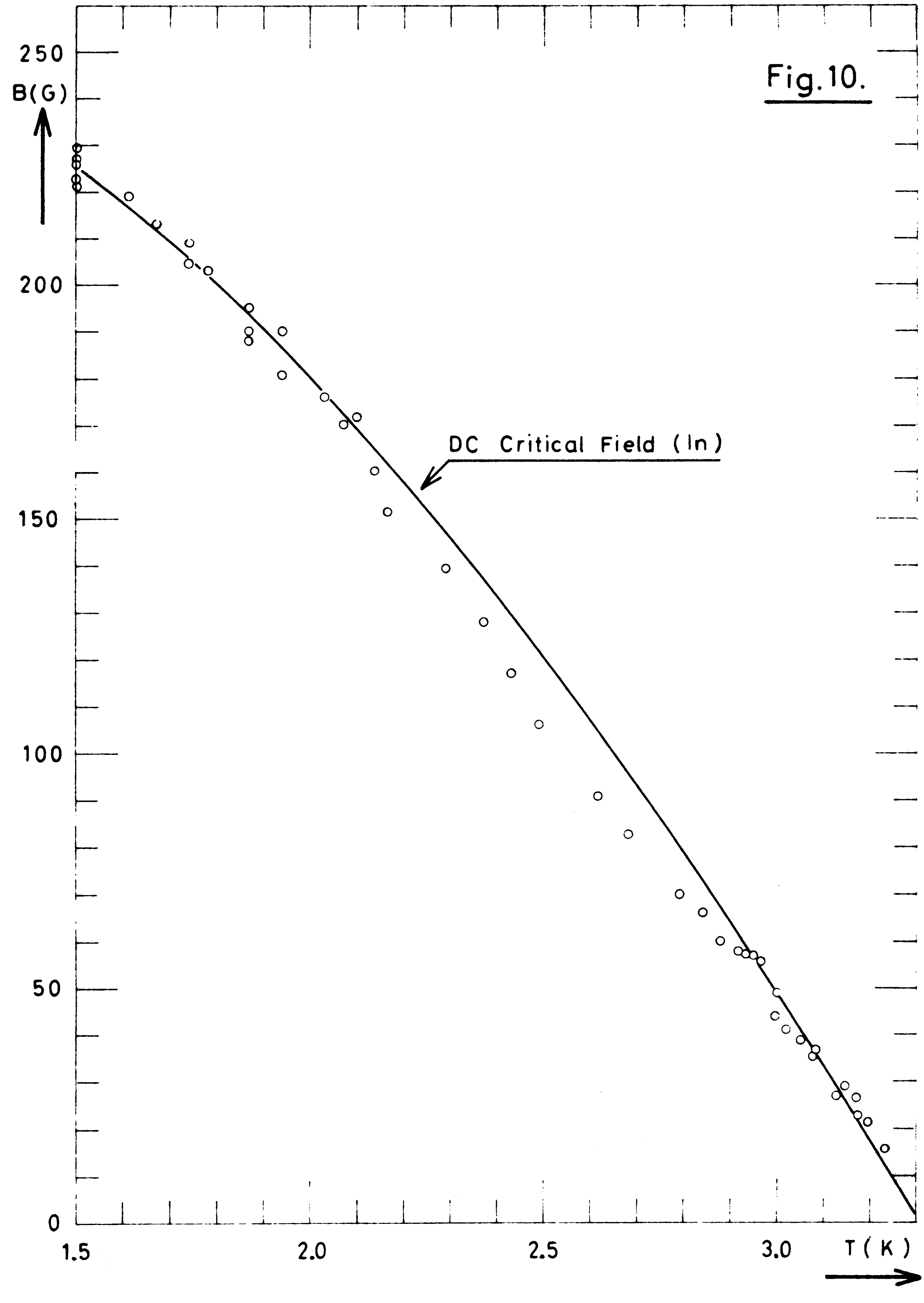

Fig. 10.

Fig. 11.

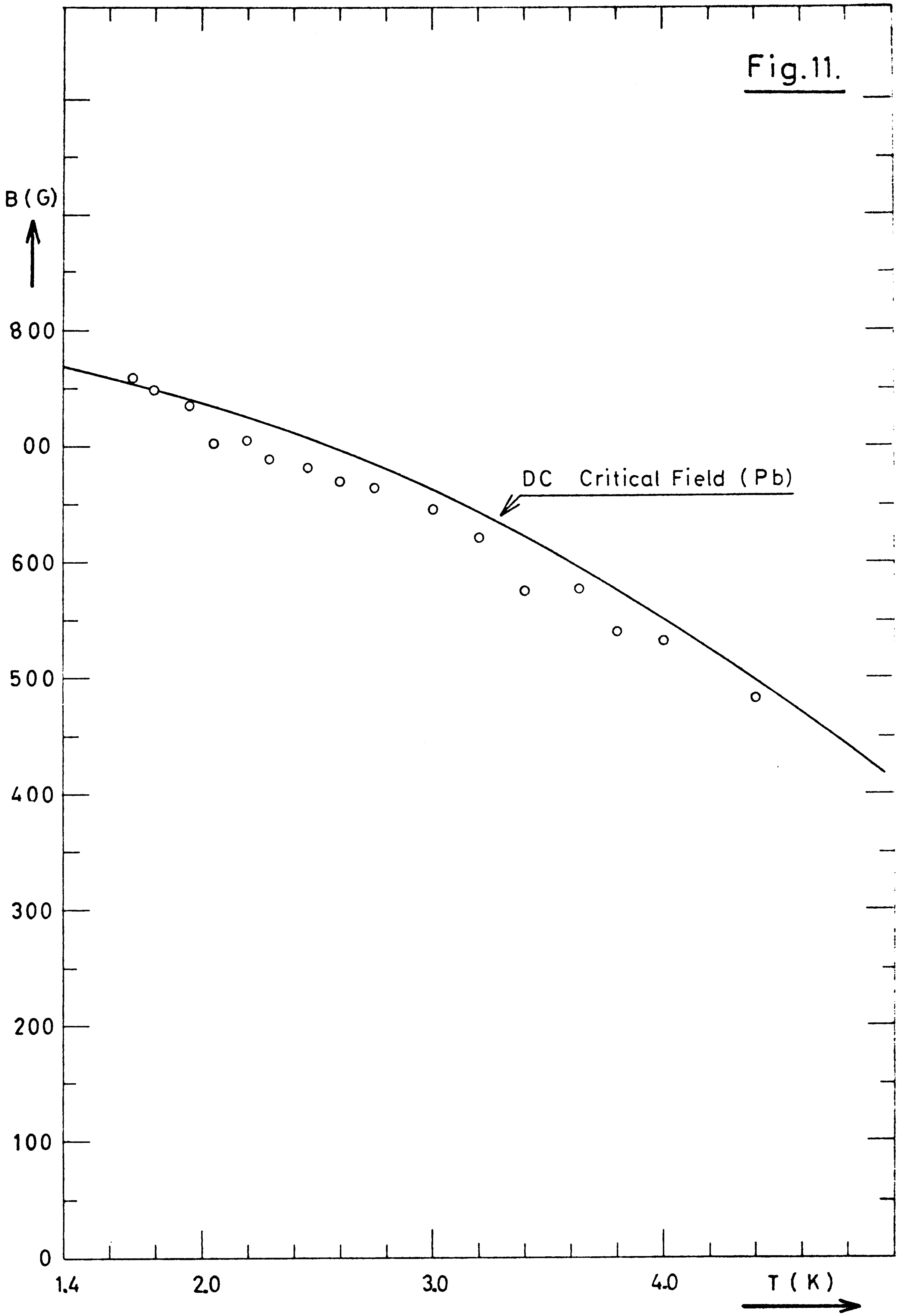

B (G)
800
00
600
500
400
300
200
100
0
DC Critical Field (Pb)
1.4
2.0
3.0
4.0
T (K)

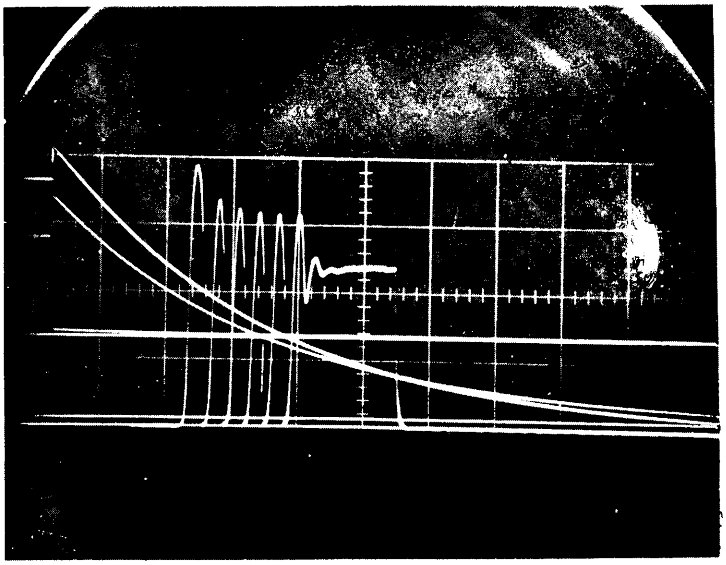

Photo 1

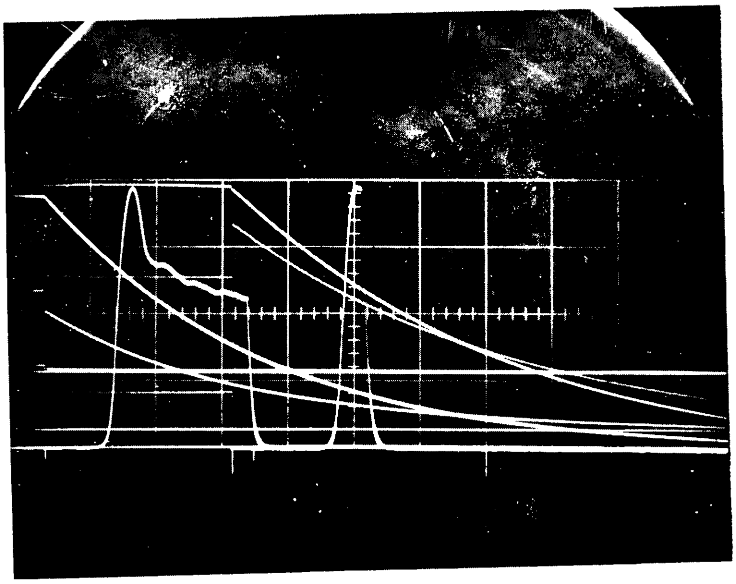

Photo 2